Letter

Chirality-inverted Dzyaloshinskii-Moriya interaction

Khalil Zakeri [1,*] Alberto Marmodoro [2,3] Albrecht von Faber [1] Sergiy Mankovsky [4] and Hubert Ebert [4]

[1]*Heisenberg Spin-dynamics Group, Physikalisches Institut, Karlsruhe Institute of Technology, Wolfgang-Gaede-Strasse 1, D-76131 Karlsruhe, Germany*
[2]*Institute of Physics, Academy of Science of the Czech Republic, Cukrovarnická 10, CZ-16253 Praha 6, Czech Republic*
[3]*New Technologies Research Centre, University of West Bohemia, CZ-30100 Pilsen, Czech Republic*
[4]*Department of Chemistry and Physical Chemistry, LMU Munich, Butenandtstrasse 11, D-81377 Munich, Germany*

The Dzyaloshinskii-Moriya interaction (DMI) is an antisymmetric exchange interaction, which is responsible for the formation of topologically protected spin textures in chiral magnets. Here, by measuring the dispersion relation of the DM energy, we quantify the atomistic DMI in a model system, i.e., a Co double layer on Ir(001). We unambiguously demonstrate the presence of a chirality-inverted DMI, i.e., a sign change in the chirality index of DMI from negative to positive, when comparing the interaction between nearest neighbors to that between neighbors located at longer distances. The effect is in analogy to the change in the character of the Heisenberg exchange interaction from, e.g., ferromagnetic to antiferromagnetic. We show that the pattern of the atomistic DMI in epitaxial magnetic structures can be very complex and provide critical insights into the nature of DMI. We anticipate that the observed effect is general and occurs in many magnetic nanostructures grown on heavy-element metallic substrates.

The exchange interaction is an inherently quantum mechanical effect, which describes the fundamental interaction between indistinguishable particles. In magnetic solids, the symmetric Heisenberg exchange interaction (HEI) is essential to understand the magnetic order [1]. In a spin Hamiltonian representation, having the form of $\mathcal{H}_{\mathrm{HEI}} = -\sum_{i \neq j} J_{ij} \mathbf{S}_i \cdot \mathbf{S}_j$, the exchange coupling parameter J_{ij}, which describes the interaction between atomic spins $\mathbf{S}_i$ and $\mathbf{S}_j$, is symmetric with respect to permutation of the atoms on sites i and j. The ferro- or antiferromagnetic interaction manifests itself in the sign of J_{ij}. Depending on the mechanism dominating the interatomic exchange interaction in a material, the coupling can be either short range, e.g., as in the case of the direct exchange or superexchange interactions, or long range, as for instance in the case of the Ruderman-Kittel-Kasuya-Yosida (RKKY) interaction [2–4], having oscillatory behavior as a function of the interatomic distance. The latter one is intrinsic for the itinerant-electron systems and may be significant in three-dimensional (3D) systems, e.g., bcc Fe [5–10], and in two-dimensional (2D) systems, e.g., ultrathin films [11,12]. Moreover, J_{ij} can change sign from positive (ferromagnetic) to negative (antiferromagnetic) as a function of the interatomic distance in an oscillatory manner [12].

In addition to HEI there exists another type of exchange interaction that is of antisymmetric nature. This interaction, which has the form of $\mathcal{H}_{\mathrm{DMI}} = \sum_{i \neq j} \mathbf{D}_{ij} \cdot \mathbf{S}_i \times \mathbf{S}_j$. is known as the Dzyaloshinskii-Moriya interaction (DMI) [13,14]. Here, the so-called DM vector $\mathbf{D}_{ij}$ is antisymmetric with respect to permutation of the sites i and j. The direction of $\mathbf{D}_{ij}$ is governed by the symmetry of the lattice [14] and determines the twist of spins. DMI is a chiral interaction and has been shown to be a consequence of spin-orbit coupling (SOC) in spin systems with broken inversion symmetry [13,14].

In the case of ultrathin magnetic films, nanostructures as well as separated magnetic atoms deposited on heavy-element metallic substrates DMI can be significant due to the strong SOC of the substrate. However, since each of these systems belong to a different dimensionality class, different interactions act on individual atomic spins, and hence the microscopic nature of the interaction responsible for the DMI is different. It has been discussed that the DMI between the deposited individual magnetic atoms may change its sign as a function of the separation distance in an oscillatory manner [15]. A similar behavior is predicted for magnetic chains deposited on stepped surfaces [16]. In the case of ultrathin magnetic films, multilayers, and nanostructures, the atomistic DMI vectors are linked to the symmetry of the underlying lattice and hence form an array of chiral vectors. In such a case the interesting feature would be that any change in the sign of the DMI vectors would lead to a chirality inversion within this array and a possible local change in the winding number $\mathcal{Q}$. Unfortunately, the experimental proof of any sign change in the DMI vectors in such planar magnets has remained elusive, since a quantitative experimental determination of the atomistic DMI vectors is challenging. It is well known that in 2D systems DMI leads to the formation of spin textures, e.g., magnetic helices [17], spirals [18], skyrmions [19,20], antiskyrmions [21], merons [22], and antimerons [23], some of which are topologically protected. For an experimental design of a specific spin texture a detailed knowledge of the fundamental magnetic interactions in such 2D systems is of prime importance. Hence, in the case of magnetic structures of itinerant electron character grown on substrates with a strong
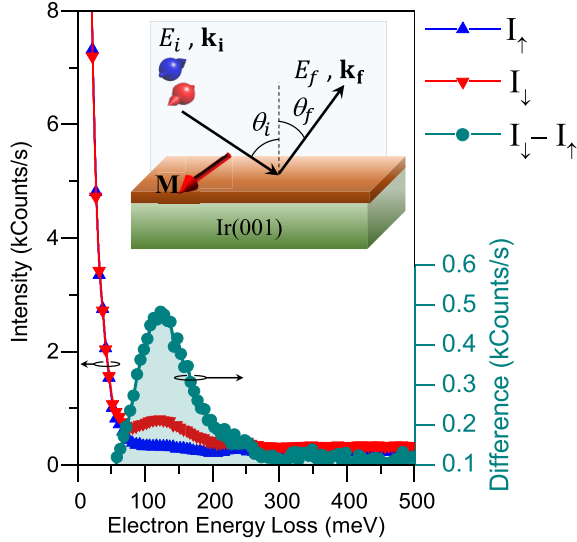
---

*khalil.zakeri@partner.kit.edu

FIG. 1. Typical SPHREEL spectra recorded at a wave vector of $Q = 0.65$ Å^{-1} on a Co double layer epitaxially grown on Ir(001). The spectra are recorded at the incident energy of $E_i = 8$ eV and at room temperature. The red and blue spectra, denoted by $I_\downarrow$ and $I_\uparrow$, are recorded with the spin polarization vector of the incident electron beam being parallel and antiparallel to the magnetization **M**, respectively. The difference spectrum $I_\downarrow - I_\uparrow$ is shown by the seagreen color. The scattering geometry is schematically illustrated in the inset. The energy and wave vector of the incident (scattered) beam are shown by E_i and $\mathbf{k_i}$ (E_f and $\mathbf{k_f}$), respectively.

SOC one may ask the following questions. (i) Is DMI in such systems similarly long ranged as HEI? (ii) Is the sign of $\mathbf{D}_{ij}$ only given by the symmetry of the lattice? (iii) Can the sign of $\mathbf{D}_{ij}$ change with interatomic distance, in a similar fashion as J_{ij}? If this is true, one would expect a chirality inversion of DMI when comparing the nearest-neighbor interaction to the interaction between spins located at a longer distances. This would provide guidelines for designing novel spin textures, e.g., atomic scale skyrmionium with $\mathcal{Q} = 0$ or more complex spin textures including skyrmions and skyrmioniums.

In this Letter we will provide answers to all these fundamental questions. We will show that the pattern of $\mathbf{D}_{ij}$ in low-dimensional itinerant magnetic structures grown on heavy-element metallic substrates can be rather complex. We introduce the magnon spectroscopy as a versatile tool to resolve such complex patterns of DMI. We provide direct experimental evidence for a change of the chirality index of DMI, which manifests itself in the asymmetry of the magnon dispersion relation. We will shed light on the origin of the observed effect and provide guidelines for quantum engineering of DMI in low-dimensional magnets on the atomic scale.

We examine an epitaxial Co double layer on Ir(001) as a representative of 2D systems. All the experimental details are provided in the Supplemental Material [24]. We have shown earlier that the presence of DMI would lead to an asymmetry in the magnon dispersion relation [25–27] and hence magnon spectroscopy provides a way to identify DMI [28,29]. The magnon dispersion relation was probed along the $\bar{\Gamma}$-$\bar{X}$ direction of the surface Brillouin zone by means of spin-polarized high-resolution electron energy-loss spectroscopy
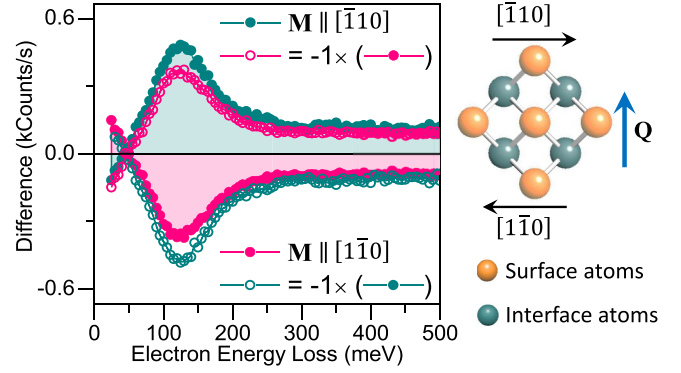

FIG. 2. Difference spectra recorded at $Q = 0.65$ Å^{-1} for the two opposite directions of magnetization, i.e., $\mathbf{M} \parallel [\bar{1}10]$ (seagreen solid circles) and $\mathbf{M} \parallel [1\bar{1}0]$ (red solid circles). In order to easily compare the spectra with different magnetization directions, the same spectra multiplied by -1 are shown as well. The magnon propagation direction (wave vector $\mathbf{Q}$) with respect to the principle directions of the Co layers and $\mathbf{M}$ is schematically sketched on the right-hand side.

(SPHREELS) [30–32]. Typical SPHREEL spectra are presented in Fig. 1. The spectra were recorded for different spin polarizations of the incoming electron beam. $I_\downarrow$ ($I_\uparrow$) represents the intensity spectrum when the spin polarization of the incoming electron beam was parallel (antiparallel) to the ground state magnetization **M**. The difference spectrum $I_\downarrow - I_\uparrow$ provides all the necessary information regarding the magnons, e.g., their energy and lifetime [33,34]. In this experiment **M** was parallel to the $[\bar{1}10]$ direction and the magnon wave vector $\mathbf{Q}$ was along the $[\bar{1}10]$ direction (see Figs. 1 and 2).

DMI lifts the degeneracy of magnons having the same value of the wave vector but opposite propagation directions. Therefore, measuring the energy asymmetry $\Delta\varepsilon(\mathbf{Q}) = \varepsilon(\mathbf{Q}) - \varepsilon(-\mathbf{Q})$ of the magnon dispersion relation provides a way to quantify the strength of DMI [26]. However, experimental determination of this asymmetry is not trivial, as probing the magnons with opposite orientations of $\mathbf{Q}$ requires a change in the scattering geometry, which may lead to unwanted effects. We have shown that a more accurate way is to perform a time-inversion experiment, keeping the scattering geometry unchanged [27]. This can be realized by reversing the direction of **M**. The energy asymmetry can, therefore, be defined as $\Delta\varepsilon(\mathbf{Q}) = \varepsilon_{\mathbf{M}\parallel[\bar{1}10]}(\mathbf{Q}) - \varepsilon_{\mathbf{M}\parallel[1\bar{1}0]}(\mathbf{Q})$, where $\varepsilon_{\mathbf{M}\parallel[\bar{1}10]}(\mathbf{Q})$ and $\varepsilon_{\mathbf{M}\parallel[1\bar{1}0]}(\mathbf{Q})$ denote the magnon energy with the wave vector $\mathbf{Q}$ when **M** is parallel to the $[\bar{1}10]$ and $[1\bar{1}0]$ direction, respectively. Figure 2 shows the difference spectrum recorded for $Q = 0.65$ Å^{-1} and for two different orientations of **M**, i.e., $[\bar{1}10]$ and $[1\bar{1}0]$.

Data presented in Fig. 2 unambiguously indicate that in this system DMI is present. However, the value of $\Delta\varepsilon$ is only about 4 meV, which seems to be rather small, at first glance. In order to shed light on the origin of this low value of $\Delta\varepsilon$ and also to further quantify the atomistic DM vectors we have probed the so-called dispersion relation of the DM energy, i.e., energy asymmetry versus wave vector $\Delta\varepsilon(\mathbf{Q})$. A summary of the results from several different experiments performed on different samples (thicknesses of 1.8, 2, and 2.4 atomic layers) is
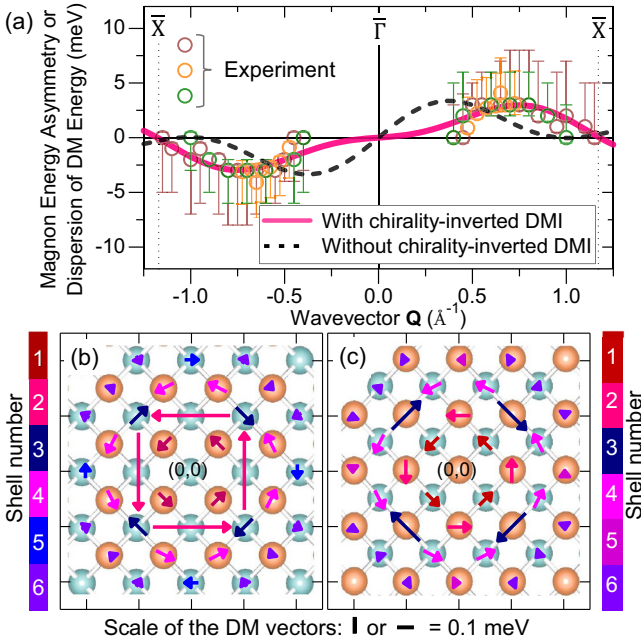
FIG. 3. (a) Dispersion relation of the DM energy $\varepsilon(\mathbf{Q})$. The experimental data are shown by the open circles. Different colors indicate the results of different (but similar) samples. The error bars represent the standard deviations in the values of $\Delta\varepsilon$. The results of *ab initio* calculations are shown by the solid red curve. The black dashed curve indicates the artificial assumption of all DMI having alike counter clockwise chirality. (b) and (c) DM vectors from *ab initio* calculations when the origin site (0,0) is located in the interface Co layer (b) and in the surface Co layer (c). In the ball representation of the Co atoms the seagreen and orange colors indicate the interface and surface layers, respectively. The color scales represent the order of nearest neighbors. The chirality index is also encoded in the color code. More red (blue) means a counterclockwise (clockwise) rotation is favored.

presented in Fig. 3. Since the quantity $\Delta\varepsilon(\mathbf{Q})$ is antisymmetric with respect to $\mathbf{Q}$, the data seem to be mirrored with respect to the origin. Note that at low wave vectors the dipolar scattering along with the large SOC of the system leads to interesting spin-dependent effects (a discussion on such effects is out of the scopes of the present Letter, see also Supplemental Note II [24]). We therefore focus on the spectra collected away from the dipolar scattering regime, where those effects are absent. Instead, we show the measurement with small steps of wave vectors. Here, the most important observations are as follows: (i) The energy asymmetry is unexpectedly low, and (ii) more importantly, the maximum and the minimum of $\Delta\varepsilon(\mathbf{Q})$ are located in the second half of the $\bar{\Gamma}$-$\bar{X}$ path. Both observations are clear evidence of a chirality-inverted DMI (see below).

We resort to first-principles calculations of DMI, in order to gain further insight into the physics of these observations [24]. Our first-principles calculations are based on the fully relativistic Korringa-Kohn-Rostoker electronic structure method [35]. Details of the scheme used to compute the above quantities within the general framework of the magnetic force theorem [36] are given in Ref. [37]. The experimental interatomic distances were used as the input of the calculations [38–42].

The calculation results are summarized in Figs. 3(b) and 3(c), where we show the DM vectors describing the antisymmetric interaction between the Co atoms only. The values are similar to the literature values for similar systems [20,21,25,43–49]. In Fig. 3(b) the interaction of a Co atom located at position (0,0) within the interface layer, adjacent to the Ir(001) surface, with the other Co atoms at position $\mathbf{R}_j$ in the same layer (seagreen color) or located in the exposed surface layer (orange color) are shown. Similarly, Fig. 3(c) displays the DMI between a Co atom located within the surface layer at (0,0) and the other Co atoms sitting at sites $\mathbf{R}_j$ either in the same layer (orange color) or located in the deeper interface layer (seagreen color). The length of each vector represents the strength of the interaction $|\mathbf{D}_{ij}|$ and their color represents their distance from the origin sites (0,0). The rotation sense of the DM vectors is also encoded in their color. The red color means that a counterclockwise rotation is favored and the blue color indicates a clockwise rotation of the DM vectors. The chirality index is defined as $c = \hat{\mathbf{D}}_{ij} \cdot \hat{\mathbf{S}}_i \times \hat{\mathbf{S}}_j$, where the hat indicates the unit vector. Its sign is therefore directly given by the direction of $\mathbf{D}_{ij}$ [50]. Looking at the data presented in Fig. 3(b) one realizes that the first-nearest-neighbor DM vectors, shown in brown color, are rather small ($D_{1,x} = D_{1,y} = -0.073$ meV). They exhibit a counterclockwise (CCW) rotation about the origin site (0,0) ($c < 0$). The second-nearest-neighbor DM vectors, shown in red color, are rather large [($D_{2,x} = -0.45, D_{2,y} = 0$) or ($D_{2,x} = 0, D_{2,y} = -0.45$) meV] and also show a CCW rotation sense ($c < 0$). The surprising result was obtained for the third nearest neighbor (dark-blue color). The DM vectors show a clockwise (CW) rotation ($c > 0$) with the components $D_{3,x} = D_{3,y} = +0.1$ meV. Interestingly, the fourth nearest neighbors favor again a CCW rotation sense ($c < 0$) but the fifth nearest neighbor DM vectors have the tendency to be of CW nature ($c > 0$). Looking at the data presented in Fig. 3(c) one can draw a similar conclusion. The only difference is that the third nearest neighbor shows a more pronounced positive chirality (CW rotation) $D_{3,x} = D_{3,y} = +0.16$ meV. Unlike the interface layer the fifth nearest neighbor exhibits also a negative chirality index ($c < 0$, CCW rotation).

Based on the values obtained from first principles, we calculated the dispersion relation of the DM energy and the results are shown by the solid red curve in Fig. 3(a) [24]. In line with the experiment one observes that the dispersion relation of the DM energy exhibits its extrema at ± 0.7 Å^{-1}. It is apparent that such an observation cannot be understood if all DMI terms possess the same chirality. This is demonstrated by the black dashed curve shown in Fig. 3(a). In such a case one must observe a rapid increase of $\Delta\varepsilon(\mathbf{Q})$ as Q increases with extrema located in the first half of the $\bar{\Gamma}$-$\bar{X}$ symmetry direction, i.e., below 0.5 Å^{-1}, and a rapid decrease at larger wave vectors. In the region of small wave vectors $\Delta\varepsilon(\mathbf{Q})$ can be approximated by terms linear with respect to Q. Hence, only if the system exhibits a chirality inversion of DMI would one observe a reduction of the DM energy in this region, as a result of competing terms with opposite signs. Note that the higher-order Heisenberg types of exchange interactions are all of a symmetric nature and hence do not appear in $\Delta\varepsilon(\mathbf{Q})$. Moreover, other interactions of chiral character are expected to be much weaker than DMI and their

contribution to $\Delta\varepsilon(\mathbf{Q})$ may be neglected (see Supplemental Note II [24]).

Our results clarify the long-standing question regarding the small micromagnetic DMI of the Co/Ir interface (cf. Refs. [51,52] and references therein), which seems to be due to cancellation effect of negative and positive terms. The overall (micromagnetic) DMI is still negative (CCW rotation) [24].

In order to shed light on the origin of the observed chirality-inverted DMI, one may start with the model by Fert and Levy for a three-site interaction [53,54]. According to this model $\mathbf{D}_{ij}$ between $\mathbf{S}_i$ and $\mathbf{S}_j$ mediated by a nonmagnetic atom sitting on site n is given by $\mathbf{D}_{ij} = \frac{D_{ij}^0}{R_{ij}} \sum_n \mathbf{R}_{in} \cdot \mathbf{R}_{jn}(\mathbf{R}_{in} \times \mathbf{R}_{jn})/(R_{in}R_{jn})^3$ [53–55]. Here, $\mathbf{R}_{in}$ and $\mathbf{R}_{jn}$ are the displacement vectors and $D_{ij}^0 = C \sin[\gamma(E_F)] \sin[k_F(R_{in} + R_{jn} + R_{ij}) + \gamma(E_F)]$, where C is a constant proportional to the SOC strength and the strength of the interaction between the magnetic sites i and j, and γ is the scattering phase shift of the electrons on site n, which, in turn, is related to the number of available d electrons and the Fermi energy E_F or wave vector k_F. The vector product determines the direction of $\mathbf{D}_{ij}$. Considering the lattice, as shown in Figs. 3(b) and 3(c), the symmetry of the pairs of the magnetic atoms remains unchanged for all the neighbors. One would therefore expect the same sign for all $\mathbf{D}_{ij}$, as given by the vector product. For $D_{ij}^0 > 0$, one would therefore expect a CCW rotation of $\mathbf{D}_{ij}$ and hence a negative chirality index ($c < 0$). However, depending on the quantities appearing in the argument of sinus functions as well as on the sign of C the prefactor D_{ij}^0 can either be positive or negative. Any change in the sign of $\mathbf{D}_{ij}$ must therefore be due to a sign change of D_{ij}^0. Conditions under which D_{ij}^0 can be positive or negative depend on the details of the electronic structures. Hence, it is not straightforward to provide simple guidelines for which system such an effect is expected (see also Supplemental Note III [24]). Moreover, one has to recall that the coupling between Co atoms at sites i and j is mediated by electrons of the surrounding atoms, both Co as well as Ir atoms, hybridized with the electrons of the interacting Co atoms [56]. The SOC-induced spin mixing as well as the itinerant nature of the electrons in the system are essential for the observed change in the chirality index of DMI via a mechanism similar to (but beyond) that of the RKKY interaction [2–4]. Interestingly, a similar behavior has also been predicted for DMI in Co/Ir/Pt(111) [45], Ru/Co/Ir(111), and Mn/Re(0001) [57] and is expected to occur in many other combinations of $3d$ magnetic films, multilayers, and nanostructures in contact with metallic substrates. Note that the observed chirality-inverted DMI reported here is different

from the layer-dependent DMI discussed in Ref. [58] (see Supplemental Note II [24]). Our analysis of J_{ij} shows that there is no direct relation between the sign of $\mathbf{D}_{ij}$ and that of J_{ij} [24], in line with the results of Ref. [45]. Therefore, not only the overlap of the electronic wave functions but also the spin mixing and orbital contribution, as a consequence of SOC, must be important [48,59]. All these effects are tightly connected to the degree of the hybridization of the electronic states of the magnetic atoms with those of the substrate atoms [47,60,61].

In conclusion, by probing the dispersion relation of the DM energy, we quantified the atomistic DMI in a model system of an ultrathin ferromagnet on a heavy-element substrate, i.e., a Co double layer epitaxially grown on Ir(001). Our detailed analysis of the DM energy dispersion showed that the pattern of the atomistic DMI in epitaxial magnetic structures can be very complex. Upon the increase of the interatomic distances DMI can change its chirality index from positive to negative and vice versa, even though the symmetry of the system is unchanged. The effect is in analogy to the oscillatory HEI in ferromagnetic metals. The phenomenon was explained by comparing the experimental results to those of *ab initio* density functional theory calculations and was attributed to the strong electronic hybridizations, the role of orbital degree of freedom, and the presence of the spin-mixed itinerant electrons. The observed complex pattern of DM vectors is a general feature across different systems and is expected to be present in many magnetic structures grown on heavy-element metallic substrates (see Supplemental Note III [24]). Beside providing insights into the microscopic origin of DMI, our results offer alternative routes to tune this fundamental interaction on the atomic scale. Moreover, our work showcases how magnon spectroscopy, which directly probes the dispersion of DM energy, can be used to quantify the atomistic DMI in great detail and experimentally identify any chirality-inverted DMI.

[1] W. Heisenberg, Zur theorie des ferromagnetismus, Z. Phys. **49**, 619 (1928).

[2] M. A. Ruderman and C. Kittel, Indirect exchange coupling of nuclear magnetic moments by conduction electrons, Phys. Rev. **96**, 99 (1954).

[3] T. Kasuya, A theory of metallic ferro- and antiferromagnetism on Zener's model, Prog. Theor. Phys. **16**, 45 (1956).

[4] K. Yosida, Magnetic properties of Cu-Mn alloys, Phys. Rev. **106**, 893 (1957).

[5] Y. O. Kvashnin, R. Cardias, A. Szilva, I. Di Marco, M. I. Katsnelson, A. I. Lichtenstein, L. Nordström, A. B. Klautau, and O. Eriksson, Microscopic Origin of Heisenberg and Non-Heisenberg Exchange Interactions in Ferromagnetic bcc Fe, Phys. Rev. Lett. **116**, 217202 (2016).

[6] M. Pajda, J. Kudrnovský, I. Turek, V. Drchal, and P. Bruno, *Ab initio* calculations of exchange interactions, spin-wave stiffness constants, and Curie temperatures of Fe, Co, and Ni, Phys. Rev. B **64**, 174402 (2001).

[7] S. V. Halilov, H. Eschrig, A. Y. Perlov, and P. M. Oppeneer, Adiabatic spin dynamics from spin-density-functional theory: Application to Fe, Co, and Ni, Phys. Rev. B **58**, 293 (1998).

[8] M. I. Katsnelson and A. I. Lichtenstein, First-principles calculations of magnetic interactions in correlated systems, Phys. Rev. B **61**, 8906 (2000).

[9] A. Szilva, M. Costa, A. Bergman, L. Szunyogh, L. Nordström, and O. Eriksson, Interatomic Exchange Interactions for Finite-Temperature Magnetism and Nonequilibrium Spin Dynamics, Phys. Rev. Lett. **111**, 127204 (2013).

[10] R. Singer, F. Dietermann, and M. Fähnle, Spin Interactions in bcc and fcc Fe beyond the Heisenberg Model, Phys. Rev. Lett. **107**, 017204 (2011).

[11] K. Zakeri, T.-H. Chuang, A. Ernst, L. Sandratskii, P. Buczek, H. Qin, Y. Zhang, and J. Kirschner, Direct probing of the exchange interaction at buried interfaces, Nat. Nanotechnol. **8**, 853 (2013).

[12] Y. Meng, K. Zakeri, A. Ernst, T.-H. Chuang, H. J. Qin, Y.-J. Chen, and J. Kirschner, Direct evidence of antiferromagnetic exchange interaction in Fe(001) films: Strong magnon softening at the high-symmetry $\overline{M}$ point, Phys. Rev. B **90**, 174437 (2014).

[13] I. Dzyaloshinsky, A thermodynamic theory of weak ferromagnetism of antiferromagnetics, J. Phys. Chem. Solids **4**, 241 (1958).

[14] T. Moriya, Anisotropic superexchange interaction and weak ferromagnetism, Phys. Rev. **120**, 91 (1960).

[15] A. A. Khajetoorians, M. Steinbrecher, M. Ternes, M. Bouhassoune, M. dos Santos Dias, S. Lounis, J. Wiebe, and R. Wiesendanger, Tailoring the chiral magnetic interaction between two individual atoms, Nat. Commun. **7**, 10620 (2016).

[16] B. Schweflinghaus, B. Zimmermann, M. Heide, G. Bihlmayer, and S. Blügel, Role of Dzyaloshinskii-Moriya interaction for magnetism in transition-metal chains at Pt step edges, Phys. Rev. B **94**, 024403 (2016).

[17] E. Y. Vedmedenko, L. Udvardi, P. Weinberger, and R. Wiesendanger, Chiral magnetic ordering in two-dimensional ferromagnets with competing Dzyaloshinsky-Moriya interactions, Phys. Rev. B **75**, 104431 (2007).

[18] M. Bode, M. Heide, K. von Bergmann, P. Ferriani, S. Heinze, G. Bihlmayer, A. Kubetzka, O. Pietzsch, S. Blügel, and R. Wiesendanger, Chiral magnetic order at surfaces driven by inversion asymmetry, Nature (London) **447**, 190 (2007).

[19] U. K. Rößler, A. N. Bogdanov, and C. Pfleiderer, Spontaneous skyrmion ground states in magnetic metals, Nature (London) **442**, 797 (2006).

[20] S. Heinze, K. von Bergmann, M. Menzel, J. Brede, A. Kubetzka, R. Wiesendanger, G. Bihlmayer, and S. Blügel, Spontaneous atomic-scale magnetic skyrmion lattice in two dimensions, Nat. Phys. **7**, 713 (2011).

[21] M. Hoffmann, B. Zimmermann, G. P. Müller, D. Schürhoff, N. S. Kiselev, C. Melcher, and S. Blügel, Antiskyrmions stabilized at interfaces by anisotropic Dzyaloshinskii-Moriya interactions, Nat. Commun. **8**, 308 (2017).

[22] X. Z. Yu, W. Koshibae, Y. Tokunaga, K. Shibata, Y. Taguchi, N. Nagaosa, and Y. Tokura, Transformation between meron and skyrmion topological spin textures in a chiral magnet, Nature (London) **564**, 95 (2018).

[23] S. Hayami and R. Yambe, Meron-antimeron crystals in non-centrosymmetric itinerant magnets on a triangular lattice, Phys. Rev. B **104**, 094425 (2021).

[24] See Supplemental Material at http://link.aps.org/supplemental/10.1103/PhysRevB.108.L100403 for detailed information, which includes Refs. [25,26,28,29,35–42,51,58,62–71].

[25] L. Udvardi and L. Szunyogh, Chiral Asymmetry of the Spin-Wave Spectra in Ultrathin Magnetic Films, Phys. Rev. Lett. **102**, 207204 (2009).

[26] K. Zakeri, Y. Zhang, J. Prokop, T.-H. Chuang, N. Sakr, W. X. Tang, and J. Kirschner, Asymmetric Spin-Wave Dispersion on Fe(110): Direct Evidence of the Dzyaloshinskii-Moriya Interaction, Phys. Rev. Lett. **104**, 137203 (2010).

[27] K. Zakeri, Y. Zhang, T.-H. Chuang, and J. Kirschner, Magnon Lifetimes on the Fe(110) Surface: The Role of Spin-Orbit Coupling, Phys. Rev. Lett. **108**, 197205 (2012).

[28] K. Zakeri, Probing of the interfacial Heisenberg and Dzyaloshinskii–Moriya exchange interaction by magnon spectroscopy, J. Phys.: Condens. Matter **29**, 013001 (2017).

[29] S. Tsurkan and K. Zakeri, Giant Dzyaloshinskii-Moriya interaction in epitaxial Co/Fe bilayers with C_{2v} symmetry, Phys. Rev. B **102**, 060406(R) (2020).

[30] K. Zakeri, Y. Zhang, and J. Kirschner, Surface magnons probed by spin-polarized electron energy loss spectroscopy, J. Electron Spectrosc. Relat. Phenom. **189**, 157 (2013).

[31] K. Zakeri and J. Kirschner, *Probing magnons by spin-polarized electrons*, in *Magnonics*, edited by S. Demokritov and A. Slavin, Topics in Applied Physics Vol. 125 (Springer, Berlin, 2013), Chap. 7, pp. 84–99.

[32] K. Zakeri, Elementary spin excitations in ultrathin itinerant magnets, Phys. Rep. **545**, 47 (2014).

[33] Y. Zhang, P. A. Ignatiev, J. Prokop, I. Tudosa, T. R. F. Peixoto, W. X. Tang, K. Zakeri, V. S. Stepanyuk, and J. Kirschner, Elementary Excitations at Magnetic Surfaces and Their Spin Dependence, Phys. Rev. Lett. **106**, 127201 (2011).

[34] Y. Zhang, T.-H. Chuang, K. Zakeri, and J. Kirschner, Relaxation Time of Terahertz Magnons Excited at Ferromagnetic Surfaces, Phys. Rev. Lett. **109**, 087203 (2012).

[35] H. Ebert, D. Ködderitzsch, and J. Minár, Calculating condensed matter properties using the KKR-Green's function method-recent developments and applications, Rep. Prog. Phys. **74**, 096501 (2011).

[36] A. I. Liechtenstein, M. I. Katsnelson, V. P. Antropov, and V. A. Gubanov, Local spin density functional approach to the theory of exchange interactions in ferromagnetic metals and alloys, J. Magn. Magn. Mater. **67**, 65 (1987).

[37] S. Mankovsky and H. Ebert, Accurate scheme to calculate the interatomic Dzyaloshinskii-Moriya interaction parameters, Phys. Rev. B **96**, 104416 (2017).

[38] K. Heinz and L. Hammer, Nanostructure formation on Ir(100), Prog. Surf. Sci. **84**, 2 (2009).

[39] Y.-J. Chen, K. Zakeri, A. Ernst, H. J. Qin, Y. Meng, and J. Kirschner, Group Velocity Engineering of Confined Ultrafast Magnons, Phys. Rev. Lett. **119**, 267201 (2017).

[40] K. Zakeri, A. Hjelt, I. V. Maznichenko, P. Buczek, and A. Ernst, Nonlinear Decay of Quantum Confined Magnons in Itinerant Ferromagnets, Phys. Rev. Lett. **126**, 177203 (2021).

[41] H. J. Qin, S. Tsurkan, A. Ernst, and K. Zakeri, Experimental Realization of Atomic-Scale Magnonic Crystals, Phys. Rev. Lett. **123**, 257202 (2019).

[42] K. Zakeri, H. Qin, and A. Ernst, Unconventional magnonic surface and interface states in layered ferromagnets, Commun. Phys. **4**, 18 (2021).

[43] F. Freimuth, S. Blügel, and Y. Mokrousov, Berry phase theory of Dzyaloshinskii–Moriya interaction and spin–orbit torques, J. Phys.: Condens. Matter **26**, 104202 (2014).

[44] J.-P. Hanke, F. Freimuth, S. Blügel, and Y. Mokrousov, Higher-dimensional Wannier interpolation for the modern theory of the Dzyaloshinskii–Moriya interaction: Application to Co-based trilayers, J. Phys. Soc. Jpn. **87**, 041010 (2018).

[45] G. J. Vida, E. Simon, L. Rózsa, K. Palotás, and L. Szunyogh, Domain-wall profiles in Co/Ir$_n$/Pt(111) ultrathin films: Influence of the Dzyaloshinskii-Moriya interaction, Phys. Rev. B **94**, 214422 (2016).

[46] M. Perini, S. Meyer, B. Dupé, S. von Malottki, A. Kubetzka, K. von Bergmann, R. Wiesendanger, and S. Heinze, Domain walls and Dzyaloshinskii-Moriya interaction in epitaxial Co/Ir(111) and Pt/Co/Ir(111), Phys. Rev. B **97**, 184425 (2018).

[47] B. Dupé, J. E. Bickel, Y. Mokrousov, F. Otte, K. von Bergmann, A. Kubetzka, S. Heinze, and R. Wiesendanger, Giant magnetization canting due to symmetry breaking in zigzag Co chains on Ir(001), New J. Phys. **17**, 023014 (2015).

[48] P. Jadaun, L. F. Register, and S. K. Banerjee, The microscopic origin of DMI in magnetic bilayers and prediction of giant DMI in new bilayers, npj Comput. Mater. **6**, 88 (2020).

[49] B. Zimmermann, G. Bihlmayer, M. Böttcher, M. Bouhassoune, S. Lounis, J. Sinova, S. Heinze, S. Blügel, and B. Dupé, Comparison of first-principles methods to extract magnetic parameters in ultrathin films: Co/Pt(111), Phys. Rev. B **99**, 214426 (2019).

[50] In order to be consistent with the micromagnetic DMI reported in the literature for Co/Ir(111) (for example, in Refs. [51,52] and references therein) we define the sign of c to be positive if the rotation of DM vectors in the plane is clockwise (CW) and negative if the rotation of DM vectors is counterclockwise (CCW).

[51] F. Kloodt-Twesten, S. Kuhrau, H. P. Oepen, and R. Frömter, Measuring the Dzyaloshinskii-Moriya interaction of the epitaxial Co/Ir(111) interface, Phys. Rev. B **100**, 100402(R) (2019).

[52] Y. Ishikuro, M. Kawaguchi, N. Kato, Y.-C. Lau, and M. Hayashi, Dzyaloshinskii-Moriya interaction and spin-orbit torque at the Ir/Co interface, Phys. Rev. B **99**, 134421 (2019).

[53] A. Fert and P. M. Levy, Role of Anisotropic Exchange Interactions in Determining the Properties of Spin-Glasses, Phys. Rev. Lett. **44**, 1538 (1980).

[54] P. M. Levy and A. Fert, Anisotropy induced by nonmagnetic impurities in CuMn spin-glass alloys, Phys. Rev. B **23**, 4667 (1981).

[55] A. Crepieux and C. Lacroix, Dzyaloshinsky–Moriya interactions induced by symmetry breaking at a surface, J. Magn. Magn. Mater. **182**, 341 (1998).

[56] L. M. Sandratskii, Insight into the Dzyaloshinskii-Moriya interaction through first-principles study of chiral magnetic structures, Phys. Rev. B **96**, 024450 (2017).

[57] S. Meyer, Complex spin structures in frustrated ultrathin films, Ph.D. thesis, Kiel University, 2020, https://macau.uni-kiel.de/receive/macau_mods_00000764.

[58] H. Yang, A. Thiaville, S. Rohart, A. Fert, and M. Chshiev, Anatomy of Dzyaloshinskii-Moriya interaction at Co/Pt interfaces, Phys. Rev. Lett. **115**, 267210 (2015).

[59] S. Kim, K. Ueda, G. Go, P.-H. Jang, K.-J. Lee, A. Belabbes, A. Manchon, M. Suzuki, Y. Kotani, T. Nakamura, K. Nakamura, T. Koyama, D. Chiba, K. T. Yamada, D.-H. Kim, T. Moriyama, K.-J. Kim, and T. Ono, Correlation of the Dzyaloshinskii–Moriya interaction with Heisenberg exchange and orbital asphericity, Nat. Commun. **9**, 1648 (2018).

[60] V. Kashid, T. Schena, B. Zimmermann, Y. Mokrousov, S. Blügel, V. Shah, and H. G. Salunke, Dzyaloshinskii-Moriya interaction and chiral magnetism in 3d-5d zigzag chains: Tight-binding model and *ab initio* calculations, Phys. Rev. B **90**, 054412 (2014).

[61] A. Belabbes, G. Bihlmayer, F. Bechstedt, S. Blügel, and A. Manchon, Hund's Rule-Driven Dzyaloshinskii-Moriya Interaction at 3d-5d Interfaces, Phys. Rev. Lett. **117**, 247202 (2016).

[62] K. Zakeri, T. Peixoto, Y. Zhang, J. Prokop, and J. Kirschner, On the preparation of clean tungsten single crystals, Surf. Sci. **604**, L1 (2010).

[63] T.-H. Chuang, K. Zakeri, A. Ernst, Y. Zhang, H. J. Qin, Y. Meng, Y.-J. Chen, and J. Kirschner, Magnetic properties and magnon excitations in Fe(001) films grown on Ir(001), Phys. Rev. B **89**, 174404 (2014).

[64] J. Küppers and H. Michel, Preparation of Ir(100)–1×1 surface structures by surface reactions and its reconstruction kinetics as determined with LEED, ups and work function measurements, Appl. Surf. Sci. **3**, 179 (1979).

[65] K. Heinz, G. Schmidt, L. Hammer, and K. Müller, Dynamics of the reconstruction process Ir(100) $1 \times 1 \to 1 \times 5$, Phys. Rev. B **32**, 6214 (1985).

[66] L. Hammer, W. Meier, A. Klein, P. Landfried, A. Schmidt, and K. Heinz, Hydrogen-Induced Self-Organized Nanostructuring of the Ir(100) Surface, Phys. Rev. Lett. **91**, 156101 (2003).

[67] D. Lerch, A. Klein, A. Schmidt, S. Müller, L. Hammer, K. Heinz, and M. Weinert, Unusual adsorption site of hydrogen on the unreconstructed Ir(100) surface, Phys. Rev. B **73**, 075430 (2006).

[68] Z. Tian, D. Sander, and J. Kirschner, Nonlinear magnetoelastic coupling of epitaxial layers of Fe, Co, and Ni on Ir(100), Phys. Rev. B **79**, 024432 (2009).

[69] M. T. Johnson, P. J. H. Bloemen, F. J. A. den Broeder, and J. J. de Vries, Magnetic anisotropy in metallic multilayers, Rep. Prog. Phys. **59**, 1409 (1996).

[70] L. Udvardi, L. Szunyogh, K. Palotás, and P. Weinberger, First-principles relativistic study of spin waves in thin magnetic films, Phys. Rev. B **68**, 104436 (2003).

[71] W. Legrand, Y. Sassi, F. Ajejas, S. Collin, L. Bocher, H. Jia, M. Hoffmann, B. Zimmermann, S. Blügel, N. Reyren, V. Cros, and A. Thiaville, Spatial extent of the Dzyaloshinskii-Moriya interaction at metallic interfaces, Phys. Rev. Mater. **6**, 024408 (2022).